

Structure of the mixed crystal $(\text{KCN})_{0.7}(\text{KBr})_{0.3}$ determined by neutron powder diffraction

J. Bouillot,* J. M. Rowe, and J. J. Rush

Institute for Materials Science and Engineering, National Bureau of Standards, Gaithersburg, Maryland 20899

(Received 8 December 1986)

Neutron powder diffraction patterns of $(\text{KCN})_{0.7}(\text{KBr})_{0.3}$ measured at various temperatures in the range 17–200 K reveal a transition at $T_c \approx 113$ K between a cubic phase above T_c and a mixed rhombohedral-monoclinic phase (below T_c), in general agreement with recent x-ray studies [K. Knorr, A. Loidl, and J. K. Kjems, *Phys. Rev. Lett.* **55**, 2445 (1985)]. In the low-temperature rhombohedral structure, the $(\text{CN})^-$ ions lie in the plane perpendicular to the threefold axis. Structural data are given and discussed.

I. INTRODUCTION

Previous structural studies of pure KCN (Refs. 1–3) have clearly established two phase transitions: (i) a first-order transition at 168 K from a cubic (NaCl) lattice where the $(\text{CN})^-$ ions are disordered, to a body-centered orthorhombic lattice in which a quadrupolar ferroelastic ordering of the $(\text{CN})^-$ ions appears along the [010] direction (cubic [110]), and (ii) a second-order transition at 83 K where the orthorhombic structure becomes primitive with an “antiferroelectric” dipolar ordering. The unit cells involved are drawn in Fig. 1. When $(\text{CN})^-$ ions are progressively replaced by Br^- ions to form the mixed compounds $(\text{KCN})_x(\text{KBr})_{1-x}$, where x ranges from 1 to 0.85, previous experiments^{4–8} have shown (i) a lowering of the transition temperature T_c , (ii) the appearance of a monoclinic structure just below T_c , and then (iii) the formation of a mixed triclinic-orthorhombic structure at lower temperature. The monoclinic (or triclinic) unit cell is shown in Fig. 1. A recent x-ray study⁹ has shown the existence of an intermediate rhombohedral structure for $x \approx 0.7$. For concentrations x lower than 0.6, no structural transition is found, and the formation of an orientational glass state has been proposed.^{10–16}

The key role of the $(\text{CN})^-$ orientations has been revealed in many elastic, quasielastic, and inelastic neutron scattering studies,^{17–19} and a microscopic model has been proposed^{20–21} to describe the effects of translation-rotation coupling. The first-order transition with a quadrupolar ordering of $(\text{CN})^-$ ions along the cubic [110] axis was shown to be governed by the softening of the transverse acoustic mode along this axis.^{18–22} The diffraction properties of an orientationally disordered state have been derived²³ on the basis of the translation-rotation coupling based on the microscopic model.

In the present paper, we focus our attention on the concentration $x = 0.7$ in an attempt to clarify the nature of the phase transitions for this concentration. The x-ray diffraction results published by Knorr *et al.*⁹ reveal an anomalous increase of the temperature factors (mean-square displacements) when approaching T_c from above, and the appearance of a pure rhombohedral phase just below T_c before the formation of the monoclinic phase. The aim of the present paper was to confirm these results

by means of neutron powder diffraction, and to study the structure of the rhombohedral phase.

II. EXPERIMENTAL

The sample was prepared by grinding solid boules of the nominal concentration ($x = 0.7$) in a mortar and pestle in a controlled atmosphere. It was then loaded into an aluminum can in a helium atmosphere and sealed with an indium O-ring. The temperature-dependent measurements were performed in a controlled-temperature displacer closed-loop helium refrigerator working from room temperature to 17 K. For temperature changes of less than 20 K, equilibrium was attained to within 1 K in less than 1 h; for larger temperature changes, longer equilibration times were required.

The neutron diffraction patterns were recorded on the five-detector high-resolution diffractometer at the National Bureau of Standards (NBS) research reactor using collimation of $20'-20'-10'$ before and after the monochromator and after the sample, respectively. The wavelength was 1.546 Å, and the 2θ angular range was 10° – 112° or 20° – 122° depending on the temperature at which the data

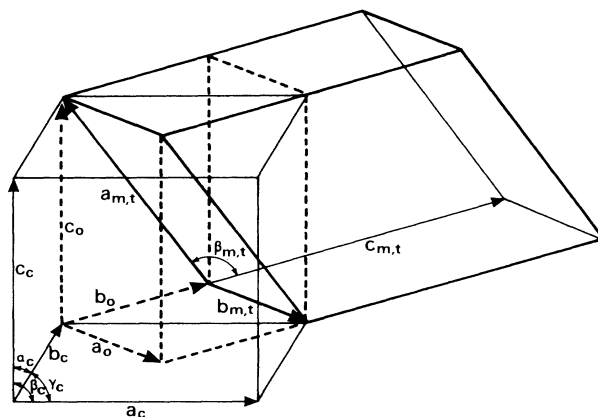


FIG. 1. Schematic representation of cubic (—), orthorhombic (---), and monoclinic (or triclinic) (—) unit cells.

were collected. A first experiment recording only a reduced part of the spectrum was performed to determine accurately the temperature at which the transition occurs.

Structural refinements were carried out using the Rietveld method, either with a single-pattern version (modified by E. Prince) for temperatures where a single phase is observed, or with a multipattern version for temperatures where a mixed structure had to be refined. In all results presented below, the temperature factor for the (CN)⁻ ions was treated as isotropic, and that for the Br⁻ ions was constrained to be equal to that for the (CN)⁻ ions. Previous experience with mixed cyanide samples, a limited exploration with the present data, and examination of the covariance matrix indicate that imposition of these constraints will have little effect on any other derived parameters.

III. DATA ANALYSIS AND DISCUSSION

A. Cubic phase, $T > 113$ K

This structure has been observed for all concentrations [pure KCN or mixed (KCN)_x(KA)_{1-x}] at sufficiently high temperature. For the present concentration $x = 0.7$ and $A = \text{Br}$ the cubic structure is observed above $T_c = 113$ K, and the main features which characterize this structure are those that have already been reported in numerous papers.²⁴⁻²⁶ They can be summarized as follows.

(1) The structure is face-centered cubic with the space group $Fm\bar{3}m$.

(2) The orientation of the (CN)⁻ ions is best described by a probability expressed in terms of symmetry-adapted spherical harmonics, with main maxima along the [111] direction and secondary maxima along the [100] directions.

The purpose of this portion of the present study was to analyze very carefully the evolution of the temperature factors (Debye-Waller factors) when approaching T_c from above.

Several refinements were performed at each temperature, starting from different initial conditions (parameters). The results are not significantly affected by such changes in the starting conditions, and the results given in Table I and Fig. 2 were obtained in the following way: The initial set of parameters, i.e., (i) CN distance; (ii) the ratio of the occupation factor along [111] to the occupation factor along [100] for the (CN)⁻ ions; (iii) parameters U , V , and W which define the resolution of the diffractometer [diffracted angle θ dependence of the full width at half maximum (Γ) according to the expression $\Gamma^2 = U \tan^2\theta + V \tan\theta + W$]; and (iv) the zero shift of the angle θ , was chosen to be identical for each temperature, the value of these parameters being the average of the best solutions precalculated at each temperature. The other parameters (lattice parameters, scale factor, temperature factors, and background) were estimated at each temperature from the same best solution mentioned above.

From the results shown in Table I, the following points should be noted.

(1) At all temperatures [111] orientations are favored over [100] orientations.

(2) The fitted values of U , V , and W do not reveal any anomalous line broadening, and, simultaneously, the line shape can be well accounted for with a Gaussian function. Therefore, neither grain-size effects nor anomalous thermal diffuse scattering have to be considered.

(3) The backgrounds are well represented by a smooth, linear function for each detector, indicating the absence of short-range order and the presence of a single, well-

TABLE I. Structural parameters of the cubic phase of (KCN)_{0.7}(KBr)_{0.3} at various temperatures. $R_{\text{nuclear}}/100 = \sum |I_B(\text{obs}) - I_B(\text{calc})| / \sum I_B(\text{obs})$, where $I_B(\text{obs})$ ($I_B(\text{calc})$) is the observed (calculated) intensity in peaks. $R_{\text{weighted}}/100 = \{ \sum w_i [y_i(\text{obs}) - y_i(\text{calc})]^2 / \sum w_i y_i^2(\text{obs}) \}^{1/2}$, where w_i is the statistical weight, and y_i refers to entire profile. R_{expected} is defined by the relation $\chi = \{ \sum w_i [y_i(\text{obs}) - y_i(\text{calc})]^2 / (N - P) \}^{1/2} = (R_{\text{weighted}}/R_{\text{expected}})$, where $N - P$ is the number of degrees of freedom. $N(hkl)$ is the proportion of (CN)⁻ ions with orientation along the $[hkl]$ axis. $\Delta(hkl)$ is the displacement of the center of the (CN)⁻ ion (with an orientation along the $[hkl]$ axis) from the center of the unit cell. U , V , and W are the parameters used to express the θ dependence of the full width at half maximum (Γ) as $\Gamma^2 = U(\tan\theta)^2 + V(\tan\theta) + W$, where the Γ is in 100th's of a degree.

		$T = 115$ K	$T = 117$ K	$T = 125$ K	$T = 150$ K	$T = 200$ K
Scale factor		5.68	5.69	6.07	6.51	6.12
a (Å)		6.4960	6.4966	6.4990	6.5065	6.5215
Zero shift (0.01°)		-2.47	-2.47	-2.47	-2.47	-2.47
$N(111)/N(100)$		2.00	2.00	2.00	2.00	2.00
$\Delta(111)$		-0.005	-0.005	-0.005	-0.005	-0.005
$\Delta(100)$		-0.008	-0.008	-0.008	-0.008	-0.008
Linewidth	U	2350	2350	2350	2350	2350
parameters	V	-1520	-1520	-1520	-1520	-1520
	W	1526	1526	1526	1526	1526
Debye-Waller	K	5.336	5.169	4.495	3.498	4.234
factors	CN	5.423	5.068	4.444	3.567	4.190
R factors:	expected	5.24	5.24	5.24	5.21	5.22
	nuclear	4.64	4.55	5.25	4.24	5.82
	weighted	6.38	6.32	5.83	6.13	6.24

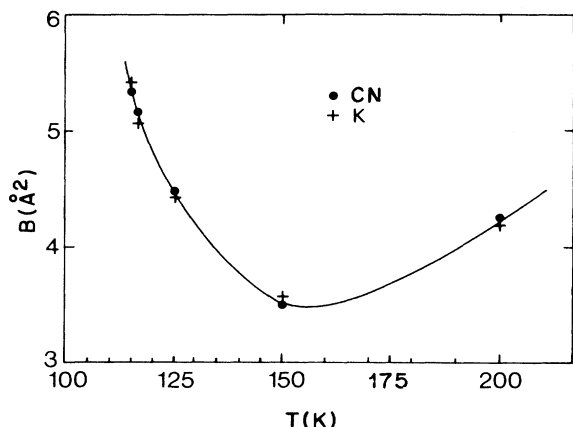


FIG. 2. Temperature dependence of the Debye-Waller factors B for the K^+ ions (●) and the $(CN)^-$ ions (+) in the temperature range where the structure is cubic.

characterized crystalline phase.

(4) The concentration has been refined and the value that gives the minimum R factor agrees with the nominal value $x = 0.7$.

In Fig. 2, which shows the temperature dependence of the temperature factors B for the $(CN)^-$ and K^+ ions, two regions can easily be observed. As the temperature is decreased from 200 K to about 160 K, both of the B factors decrease, as is expected from the normal temperature dependence of mean-square displacements. However, from about 160 K to the transition temperature estimated at 113 K, the temperature dependence of the B factors is reversed, indicating an increase of the atomic mean-square displacements, which are strongly correlated with the softening of the elastic constant C_{44} . No special divergence of the B factors is observed as T_c is approached, and the B factors (mean-square displacements) increase by a factor of approximately 1.5 from the minimum value at $T = 160$ K. This is in good agreement with the results of Ref. 9, which does not give results for the B factors, but from which a ratio of approximately 1.3 can be inferred. Since the results of Ref. 9 are based on only one weak (620) reflection, this agreement must be considered satisfactory. In fact, if we convert the B factor given for K^+ in Table I at $T = 113$ K to a mean-square displacement $\langle u^2 \rangle = B/4\pi^2$, the resultant value for the displacement is 11% of the near-neighbor distance, in excellent agreement with the results of Ref. 9, and in general agreement with calculations based on a microscopic model Ref. 27.

B. $T < 113$ K

The measurements performed by Knorr and Loidl⁷ reveal a transition from a cubic to a monoclinic structure for concentrations x in the range 0.85–0.95, and a transition from cubic to rhombohedral, followed by a transition to the monoclinic phase for concentrations ranging from $x = 0.6$ to $x = 0.8$. This result is based on the observation of the splitting of the (220) reflection recorded by x-ray

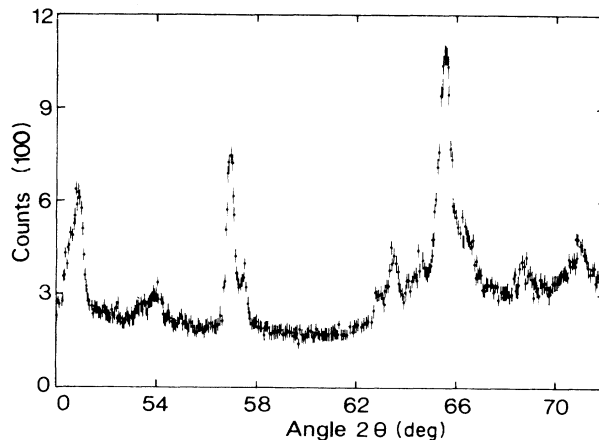


FIG. 3. Part of the measured diffraction pattern at $T = 17$ K which shows the nonlinear background.

diffraction. The monoclinic structure has been intensively discussed in previous papers,^{28,29} but the details of the rhombohedral structure have not been reported.

For the present sample with $x = 0.7$, a change of structure is clearly observed at 113 K, as indicated by the appearance of many new reflections in the neutron-diffraction pattern. This transition temperature corresponds to that found for $x = 0.73$ in Ref. 9, rather than to that found for $x = 0.7$ in Ref. 7. We do not attribute great significance to this discrepancy, since the value of x quoted for the present sample is nominal. In fact, there may well be composition gradients in the present sample, which could account for the observed coexistence of the monoclinic and rhombohedral phases at all temperatures below the transition temperature. The diffraction pattern does not show any further changes indicative of further transformations, at least for temperatures above 17 K. In order to study the details of the structures below T_c , we have measured complete diffraction patterns at 110, 105, 100, and 17 K. This last temperature, which gives the best resolution between neighboring reflections, was used to make the first detailed refinements. Figure 3 shows part of the diffraction pattern recorded at this temperature. The first result to be noted is the complex, non-linear shape of the background. This suggests that parts of the sample may not have well-characterized structures, i.e., that the sample may not have transformed homogeneously, and that there may be a large amount of short-range order.

The problem of indexing the observed lines in a powder diffraction experiment cannot be easily solved in general, but the following procedure yielded a successful solution.

(1) The 24 well-resolved lines observed could not be indexed with the assumption of a monoclinic, a rhombohedral, triclinic, nor a mixed triclinic-orthorhombic structure, all of which phases have been previously observed for other concentrations. In addition, a program designed to index unknown single-phase patterns could never index more than 20 of the 24 well-defined lines. Thus, the assumption of a new mixed phase was necessary.

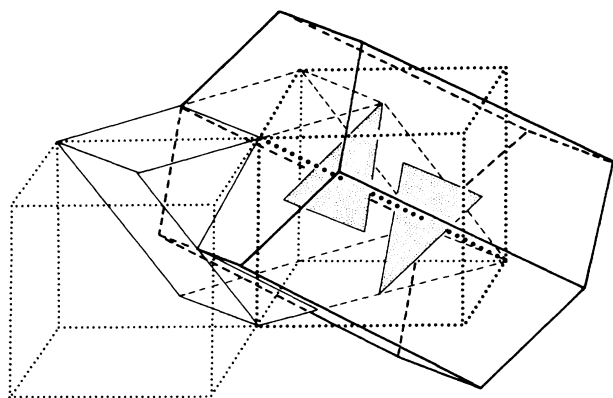


FIG. 4. Schematic representation of the rhombohedral lattice drawn by means of the hexagonal unit cell (—) or (---) in the framework of the cubic (· · ·) or (· · ·) and the monoclinic (— or ---) lattices.

(2) The first satisfactory indexing was based on the coexistence of two similar monoclinic phases with somewhat different lattice parameters, thus giving rise to different lines, i.e., $a = 7.7228 \text{ \AA}$, $b = 4.6622 \text{ \AA}$, $c = 9.0065 \text{ \AA}$, $\alpha = 90^\circ$, $\beta = 122.933^\circ$, and $\gamma = 90^\circ$ for the monoclinic-1 phase, and $a = 7.6092 \text{ \AA}$, $b = 4.6066 \text{ \AA}$, $c = 9.1640 \text{ \AA}$, $\alpha = 90^\circ$, $\beta = 122.432^\circ$, and $\gamma = 90^\circ$ for the monoclinic-2 phase.

The corresponding refinement gave a (nuclear) R factor (see definition in Table I) of the order of 11, with two nonzero calculated intensities that were not observed. No simple relations were found to correlate the basic vectors that define the two different monoclinic unit cells. Therefore the only physical conclusion was that one of those two monoclinic lattices must have a higher symmetry.

A careful study of both monoclinic lattices showed that one of them (monoclinic 1), has in fact hexagonal symmetry, with the $[001]$ direction parallel to a $[111]$ direction of

TABLE II. Structural parameters for the rhombohedral phase of $(\text{KCN})_{0.7}(\text{KBr})_{0.3}$ at 17 K. See Table I for definitions of R factors. Note: The $(\text{CN})^-$ ions are oriented perpendicular to the c axis, centered at $00\frac{1}{2}$, and the space group $R\bar{3}m$ requires occupation of the equivalent positions $x0\frac{1}{2}$, $0x\frac{1}{2}$, $xx\frac{1}{2}$, $\bar{x}0\frac{1}{2}$, $0\bar{x}\frac{1}{2}$, and $\bar{x}\bar{x}\frac{1}{2}$. In these positions, x is given below for C or N, and this equivalence replicates the C or N position six times. When combined with the large values of B given below, this results in an almost isotropic distribution of $(\text{CN})^-$ orientations in the basal plane. Line-shape parameters: $U = 10\,722$, $V = -4359$, $W = 1752$. Lattice parameters: $a = b = 4.6615 \text{ \AA}$, $c = 10.8522 \text{ \AA}$, $\alpha = \beta = 90^\circ$, R factors: $R_{\text{expected}} = 10.3$, $R_{\text{nuclear}} = 10.0$, $R_{\text{weighted}} = 13.1$.

	x	y	z	B
K	0	0	0	2.92
C	0.1182	0	0.5	6.39
N	-0.1182	0	0.5	6.39
Br	0	0	0.5	6.39

the high-temperature cubic lattice. Further attempts showed that only the $[111]$ cubic direction, which corresponds to the $[20\bar{1}]$ direction in the monoclinic lattice, allows the hexagonal symmetry. Figure 4 shows how the hexagonal unit cell is built from the monoclinic and cubic lattices. The hexagonal lattice parameters are

$$a = b = 4.6615 \text{ \AA}, \quad c = 10.8522 \text{ \AA},$$

$$\alpha = \beta = 90^\circ, \quad \gamma = 120^\circ.$$

The best refinement ($R_{\text{weighted}} = 13$, $R_{\text{nuclear}} = 10$) was obtained with a mixed phase based on the monoclinic-2 lattice with the space group Cc and the hexagonal lattice

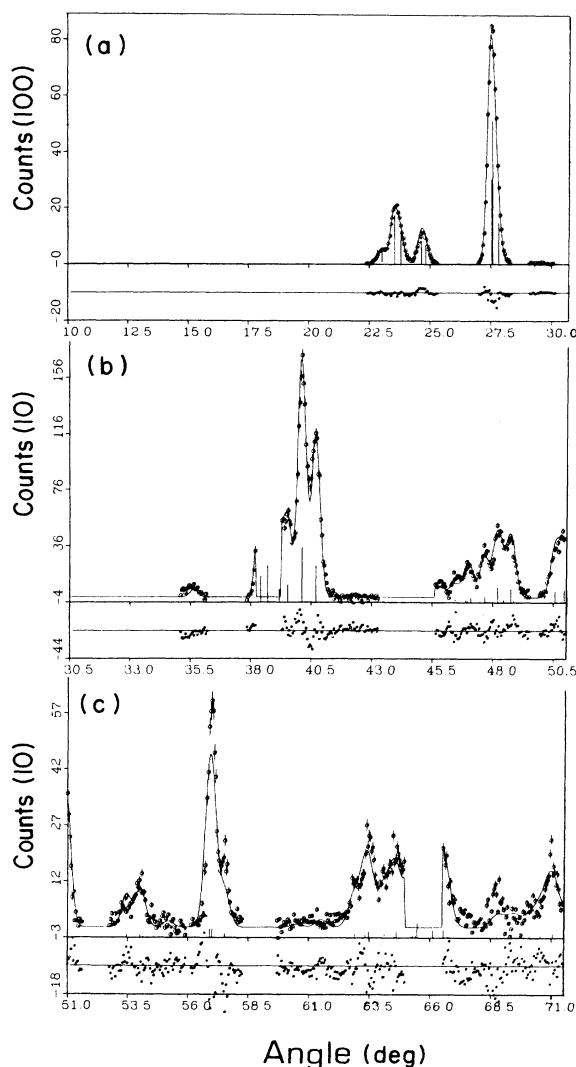


FIG. 5. Observed (circles) and calculated (solid line) diffraction patterns for $(\text{KCN})_{0.7}(\text{KBr})_{0.3}$ at $T = 17 \text{ K}$. Only a part of the angular range is shown. Gaps in the data correspond to regions of the pattern where the diffraction lines of the aluminum sample can be observed, which are excluded from all fits. (a), (b), and (c) show different angular regions of the data, recorded on different detectors.

with the rhombohedral space group $R\bar{3}m$. The observed and calculated spectra are shown in Fig. 5. The structural parameters related to the monoclinic phase are very close to those already obtained for higher concentrations x , and the structural parameters describing the rhombohedral phase are given in Table II. The most important result is the orientation of the $(\text{CN})^-$ ion, which is found to be perpendicular to the c hexagonal axis ($[111]$ direction in the cubic lattice). All other $(\text{CN})^-$ orientations give a much larger R factor (R_{weighted} of the order of 20). The atomic distances are within the usual limits. The large B factors shown in Table II, combined with the requirements of the space group for equivalent positions (see note after Table II), are only consistent with almost complete disorder of the $(\text{CN})^-$ ions in the basal plane. This result can also be seen by derivation and inspection of the Fourier map, which reveals an almost circular distribution of orientations of the $(\text{CN})^-$ ion in the basal plane around the mean crystallographic of the ion center at $00\frac{1}{2}$.

Using this solution to the observed pattern at 17 K, the data obtained at 100, 105, and 110 K were refined with the mixed-phase program. The refinements for these data were much worse than that obtained for 17 K, mainly as a result of the increased overlap of the peaks arising from the monoclinic and rhombohedral phases. This overlap led to great difficulty in the determination of the lattice parameters for the two phases, and the fits were often unstable. In order to overcome this problem, the lattice parameters for the two phases were determined from a subset of well-resolved lines, and the values found were then fixed in the subsequent refinements. In all cases, the best results were obtained with the atomic positions determined at 17 K and given in Table II. The lattice parameters a_r and c_r obtained for the rhombohedral phase by this procedure are shown in Fig. 6. For comparison, $a_r\sqrt{6}$, which is the value that c_r would have if the lattice were cubic, is also shown. As can be seen from the figure, c_r is always less than $a_r\sqrt{6}$, indicating that this axis is compressed compared to its value in a cubic lattice, i.e., the body diagonal of the cubic lattice is compressed. This distortion of the cubic cell favors $(\text{CN})^-$ orientations perpendicular to this axis. The distortion is a monotonic function of the temperature, decreasing to zero as the transition is approached from below, apparently in a continuous manner. The rhombohedral lattice can be de-

scribed as a distorted cubic lattice, with three equal T_{2g} shears. The value of this shear determined from the present results decreases from 3% at $T = 17$ K to 0.3% at $T = 100$ K. This latter value should be compared to the value of 3% at $T = 97$ K quoted in Ref. 7.

IV. DISCUSSION

The results for the cubic structure, which are well reproduced using only Gaussian line shapes, are in good agreement with earlier results. Whatever the fitting process used, the temperature factors start increasing with decreasing temperature at about 50 K above the transition temperature. The corresponding mean-square displacement of the atoms is increased over its minimum value by a factor of approximately 2 when the temperature T_c is approached. The present experiment was not performed with adequate temperature control to explore the divergence of the mean-square displacements in a detailed fashion as T_c is approached, but the agreement of the present results with previous measurements and calculations gives added weight to the conclusions of Ref. 9.

Below T_c the mixed phase (monoclinic and rhombohedral) gives rise to the following comments. (i) The R factor could be easily improved by using a resolution function (full width at half maximum) with a more complicated θ dependence than the usual one, which is expressed as $\Gamma^2 = U \tan^2\theta + V \tan\theta + W$. Indeed, the comparison between observed and calculated reflected lines shows a discrepancy for Γ which may be related to an anisotropy in the crystalline quality of the sample. In addition, some observed reflections have shoulders characteristic of strong strains in the lattice, and for these reflections the Gaussian shape is not well suited. (ii) Within the diffractometer resolution and the accuracy of the temperature (the powdered sample, in a 5-cm-high cylinder, is in a temperature gradient of the order of 1 K), the rhombohedral phase is never observed alone in the present study, i.e., without the monoclinic structure, in contrast to the results of Knorr *et al.*⁹

Although it is impossible to state definitively the origin of the discrepancy between our observation of only mixed monoclinic and rhombohedral structures, and the observation of a single rhombohedral phase in Ref. 9, we believe that this may be related to the different state of strain in our samples than in those used in the x-ray studies. There is direct evidence from the observed diffraction patterns of strains in our samples, and it is well known that such effects have a strong influence on the phase transitions in alkali cyanides and alkali-cyanide-alkali-halide mixtures. Additional support for this hypothesis is contained in the work of DeRaedt *et al.*,³⁰ where it is shown that there are terms in the Hamiltonian that depend explicitly on the sample size and shape. These terms will have little effect on the dynamic or structure above T_c , but will play an important role in the formation of the low-temperature structures. However, since the present sample was not well characterized with respect to concentration and concentration gradients, it is also possi-

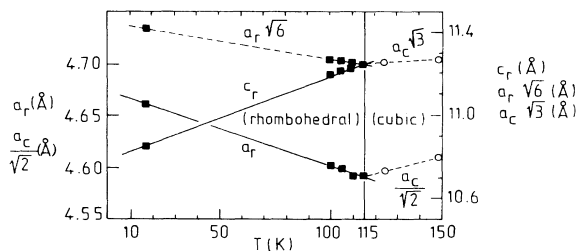


FIG. 6. Temperature dependence of the lattice parameters a_r and c_r of the rhombohedral phase. The cubic equivalents are also shown for comparison.

ble that these effects may also be responsible for the observed discrepancies. In spite of these caveats, we believe that the structure derived here for the rhombohedral phase in a mixed-phase region is representative of that in the actual equilibrium single-phase region. In particular, the orientation of the $(\text{CN})^-$ ion, which is totally orientationally disordered in a plane perpendicular to the three-fold axis, should not be strongly affected by the mixed-phase nature of our samples. This structure reveals yet another possibility for orientational disorder of $(\text{CN})^-$

ions, and illustrates again the richness of detail to be found in the alkali-cyanide-alkali-halide systems.

ACKNOWLEDGMENTS

The authors would like to thank A. Santoro, V. Himes, and A. Mighell for useful discussions on the indexing of the observed patterns. We also thank J. J. DeYoreo and R. O. Pohl for providing the sample used in these measurements.

*On leave from the Institut Laue Langevin, Grenoble, France.

Permanent address: Institut Universitaire de Technologie, 9 Rue de l'Arc en Ciel, 74019 Annecy Cedex, France.

¹T. Matsuo, H. Suga, and W. Seki, *Bull. Chem. Soc. Jpn.* **41**, 583 (1968).

²J. M. Bijvoet and J. A. Lely, *Rech. Trav. Chem. Pay Bas Belg.* **59**, 908 (1940).

³J. M. Rowe, J. J. Rush, and E. Prince, *J. Chem. Phys.* **66**, 5147 (1977).

⁴F. Luty, in *Defects in Insulating Crystals*, edited by V. M. Turkevich and K. K. Shvarts (Springer-Verlag, Berlin, 1981), pp. 69-89.

⁵G. S. Parry, *Acta Crystallogr.* **15**, 601 (1962).

⁶J. M. Rowe, J. J. Rush, and S. Susman, *Phys. Rev. B* **28**, 3506 (1983).

⁷K. Knorr and A. Loidl, *Phys. Rev. B* **31**, 5387 (1985).

⁸J. M. Rowe, J. Bouillot, J. J. Rush, and E. Luty, *Physica* **136B**, 498 (1986).

⁹K. Knorr, A. Loidl, and J. K. Kjems, *Phys. Rev. Lett.* **55**, 2445 (1985).

¹⁰J. M. Rowe, J. J. Rush, D. G. Hinks, and S. Susman, *Phys. Rev. Lett.* **43**, 1158 (1979).

¹¹A. Loidl, R. Feile, and K. Knorr, *Phys. Rev. Lett.* **48**, 1263 (1982).

¹²A. Loidl, M. Muller, G. McIntyre, K. Knorr, and H. Jex, *Solid State Commun.* **54**, 307 (1985).

¹³K. Knorr and A. Loidl, *Z. Phys. B* **46**, 219 (1982).

¹⁴S. Bhattacharya, S. R. Nagel, L. Fleishman, and S. Susman,

Phys. Rev. Lett. **48**, 1267 (1982).

¹⁵R. Feile, A. Loidl, and K. Knorr, *Phys. Rev. B* **26**, 6875 (1982).

¹⁶A. Loidl, R. Feile, K. Knorr, and J. K. Kjems, *Phys. Rev. B* **29**, 6052 (1982).

¹⁷S. Haussuhl, *Solid State Commun.* **13**, 147 (1973).

¹⁸J. M. Rowe, J. J. Rush, E. Prince, and N. J. Chesser, *Ferroelectrics* **16**, 107 (1977).

¹⁹J. M. Rowe, J. J. Rush, and N. J. Chesser, *Phys. Rev. Lett.* **40**, 455 (1978).

²⁰K. H. Michel and J. Naudts, *Phys. Rev. Lett.* **39**, 212 (1977); *J. Chem. Phys.* **67**, 547 (1977).

²¹K. H. Michel, *Z. Phys.* **54**, 129 (1984).

²²C. W. Garland, J. Z. Kwiecien, and J. C. Damien, *Phys. Rev. B* **25**, 5818 (1982).

²³K. H. Michel and J. M. Rowe, *Phys. Rev. B* **22**, 1427 (1980).

²⁴N. Elliott and J. Hastings, *Acta Crystallogr.* **14**, 1018 (1981).

²⁵D. L. Price, J. M. Rowe, J. J. Rush, E. Prince, D. G. Hinks, and S. Susman, *J. Chem. Phys.* **56**, 3697 (1972).

²⁶J. M. Rowe, D. G. Hinks, D. L. Price, S. Susman, and J. J. Rush, *J. Chem. Phys.* **58**, 2039 (1973).

²⁷K. H. Michel and J. M. Rowe, *Phys. Rev. B* **32**, 5827 (1985).

²⁸A. Cimino, G. S. Parry, and A. R. Ubbelohde, *Proc. R. Soc. London. Ser. A* **252**, 445 (1959).

²⁹C. S. Parry, *Acta Crystallogr.* **15**, 601 (1962).

³⁰B. DeRaedt, K. Binder, and K. H. Michel, *J. Chem. Phys.* **75**, 2977 (1981).